TECHNICAL RESEARCH REPORT

Poles and Zeros for Sampled-Data Duty-Ratio-to-Output
Dynamics of Buck and Boost Converters

by C.-C. Fang

T.R. 99-6

TECHNICAL RESEARCH REPORT

Poles and Zeros for Sampled-Data Duty-Ratio-to-Output
Dynamics of Buck and Boost Converters

by C.-C. Fang

T.R. 99-6

ISR
INSTITUTE FOR SYSTEMS RESEARCH

Poles and Zeros for Sampled-Data Duty-Ratio-to-Output Dynamics of Buck and Boost Converters

Chung-Chieh Fang *
Department of Electrical Engineering
National Taiwan University
Taipei 106, TAIWAN

Manuscript: Jan. 25, 1999

Abstract

Poles and zeros for sampled-data models of buck and boost converters are derived analytically for the first time (to the author's knowledge). Both continuous conduction mode (CCM) and discontinuous conduction mode (DCM) are considered. Comparisons are made with the corresponding results derived from the averaged model. For poles, the two models give similar results except in the DCM operation. For zeros, however the two models give quite different results. The zero obtained for the sampled-data model differs from that obtained for the averaged model. The zero derived from the sampled-data model depends on the switching frequency and duty ratio, as well as on the modulation scheme. For the buck converter in CCM, a single real zero exists even if the equivalent series resistance (ESR) is not modeled. Inclusion of the ESR in the model results in shifting the zero to the right in the complex plane. The zero can be unstable with or without the ESR being modeled. Undershoot is not observed because the zero is less than 1. For the boost converter in CCM, only one zero exists and this zero can be stable when the duty ratio is small. For the buck or boost converter in DCM, only one pole exists and there is no zero. The phase of the frequency response can go beyond -90 degree.

1 Introduction

A DC-DC converter consists of a power stage and a controller, as shown in Fig. 1. The most commonly used control signal is duty ratio (also called duty cycle). To design the controller, it

---

is essential to have a good model of the power stage. The open-loop poles and zeros can then be derived.
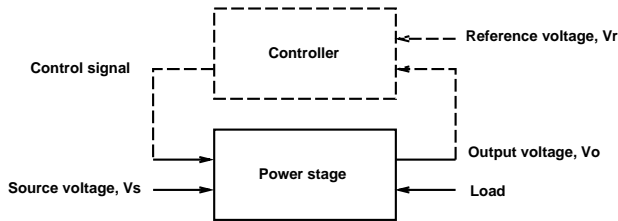
Figure 1: System diagram of a DC-DC converter

In this paper, poles and zeros for sampled-data models of buck and boost converters are derived analytically for the first time (to the author's knowledge). This work employs recent work of the author on sampled-data modeling and analysis of PWM DC-DC converters [1, 2, 3]. Knowledge of pole and zero locations is useful for discrete-time control design of DC-DC converters [4, 5, 6]. It has been seen in [3] that the sampled-data model gives a description of the dynamics of PWM DC-DC converters that is more accurate than the continuous-time state space averaged model [7, 8]. The sampled-data model is also systematic and can be written readily for a variety of models. For example, PWM DC-DC converters under current mode control or in discontinuous-conduction mode (DCM) can be easily modeled by the sampled-data approach.

In this paper, comparisons are made between the sampled-data and the averaged models. For poles, the two models give similar results except in the DCM operation. For zeros, however, the two models give quite different results.

Take the zero of the buck and boost converters in continuous-conduction mode (CCM), for example. The following statements reflect commonly held perceptions about the open-loop zeros of the state space averaged model in continuous-conduction mode (CCM): (In a continuous-time linear system, a zero in the right half of the complex plane (RHP) is called unstable. In a discrete-time linear system, a zero outside the unit circle is called unstable.)

1. The zeros are independent of the switching frequency [9, for example].

2. With the same duty ratio, the zeros in leading-edge modulation (LEM) and the zeros in trailing-edge modulation (TEM) are the same. (However, the zeros can differ in LEM and TEM if a discrete-average model [10] is used.)

3. A buck converter model without an equivalent series resistance (ESR) does not have a zero. If an ESR of value R_c is modeled, then the model has a a stable zero. The zero is at $-1/R_cC$, which is independent of the duty ratio [11, for example].

4. The boost converter model always has an unstable zero at $V_s/(LI_L)$ [12]. If an ESR of value R_c is modeled, then an additional (stable) zero occurs at $-1/R_cC$ [13].

The conclusions above will be shown not to hold for the sampled-data model. Observations that will be made using the sampled-data model include the following. In the sampled-data model, the zero depends on the switching frequency and duty ratio, as well as on the modulation scheme (viz., TEM or LEM). For the buck converter in CCM, a zero exists even if the ESR is not modeled. Inclusion of the ESR in the model results in shifting the zero to the right in the complex plane. The zero can be unstable with or without the ESR being modeled. For the boost converter in CCM, only one zero exists and this zero can be stable when the duty ratio is small.

The remainder of the paper is organized as follows. In Section 2, some basic concepts necessary for the paper are reviewed. In Section 3, the sampled-data duty-ratio-to-output transfer functions derived in [3] for general PWM DC-DC converters are given. In Section 4, poles and zeros for buck converters in CCM are derived. In 5, poles and zeros for boost converters in CCM are derived. In Section 6, the single pole of buck and boost converters in DCM is derived. In Section 7, three illustrative examples taken from the literature are given. Conclusions are collected in Section 8.

2 Preliminaries

In this section, some basic concepts necessary for the paper are reviewed.

3

2.1 PWM DC-DC Converter Dynamics

A PWM converter includes a controlled switch, a diode, and an LC filter. Generally the circuit topology is designed to prevent the switch and the diode from being on together and the switch is turned on and off once in each switching cycle. Thus there are at most three stages (controlled switch on and diode off, off-on, and off-off) in each switching cycle. These three stages are denoted as follows ON stage (controlled switch on and diode off), OFF stage (switch off and diode on), and FF stage (switch off and diode off).

Take the state of the converter to be $x := (\sqrt{L}i_L, \sqrt{C}v_C)$, i.e. scaled inductor current and capacitor voltage. Let the source voltage be a constant V_s, and denote the output voltage as v_o. In each stage, the system has linear dynamics:

$$
\begin{aligned}
\dot{x} &= A_i x + B_i V_s \\
v_o &= E_i x
\end{aligned}
\tag{1}
$$

where $i \in \{1, 2, 3\}$.

In continuous conduction mode (CCM), the inductor current never drops to zero, so the switch and the diode are never off together and there are only two stages in one switching cycle. In discontinuous conduction mode (DCM), the inductor current drops to zero and remains zero until the next cycle begins. There are therefore three stages in this mode.

Switch on and off sequence can also be different in different schemes. In trailing-edge modulation (TEM), the switch is designed to be on first in a cycle. Thus stage 1 is an ON stage and stage 2 is an OFF stage (i.e., $A_1 = A_{\mathrm{ON}}$, $A_2 = A_{\mathrm{OFF}}$, etc). In leading-edge modulation (LEM), the switch is designed to be off first in a cycle. These two schemes are illustrated in Fig. 2.

The following notation are used in the paper:

$$
f_s = \frac{1}{T} \qquad \text{(switching frequency)}
\tag{2}
$$

$$
\omega_s = 2\pi f_s \qquad \text{(angular switching frequency)}
\tag{3}
$$

$$
\omega_0 = \frac{1}{\sqrt{LC}} \qquad (LC \text{ resonant frequency})
\tag{4}
$$

4
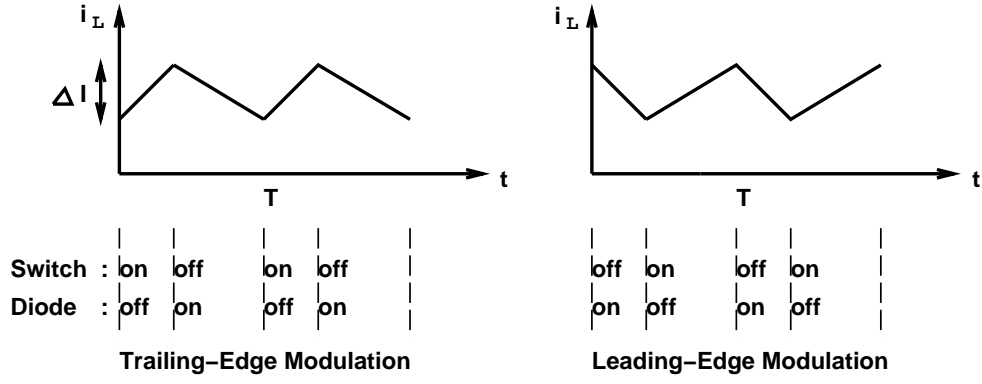
Figure 2: Trailing-edge and leading-edge modulations

$$\omega_l = \frac{R_c}{L} \tag{5}$$

$$\omega_c = \frac{1}{RC} \tag{6}$$

$$\omega_e = \frac{1}{R_c C} \tag{7}$$

$$\omega = \sqrt{\omega_0^2 - (\frac{\omega_c - \omega_l}{2})^2} \tag{8}$$

$$\kappa = \frac{R}{R + R_c} \tag{9}$$

Here $\omega_0 > |\omega_c - \omega_l|/2$ is assumed. For $R_c = 0$, one has $\omega_l = 0$, $\omega_e = \infty$, and $\kappa = 1$.

2.2   Buck Converter

The buck converter of interest in the paper is shown in Fig. 3. The matrices in Eq. (1) at each stage are

$$
\begin{aligned}
A_{\mathrm{ON}} &= A_{\mathrm{ON}} = \kappa \begin{bmatrix} -\omega_l & -\omega_0 \\ \omega_0 & -\omega_c \end{bmatrix} & A_{\mathrm{FF}} &= \kappa \begin{bmatrix} 0 & 0 \\ 0 & -\omega_c \end{bmatrix} \\
B_{\mathrm{ON}} &= \begin{bmatrix} \frac{1}{\sqrt{L}} \\ 0 \end{bmatrix} & B_{\mathrm{OFF}} &= B_{\mathrm{FF}} = \begin{bmatrix} 0 \\ 0 \end{bmatrix} \\
E_{\mathrm{ON}} &= E_{\mathrm{OFF}} = E_{\mathrm{FF}} = \kappa \begin{bmatrix} \frac{R_c}{\sqrt{L}} & \frac{1}{\sqrt{C}} \end{bmatrix}
\end{aligned}
\tag{10}
$$

5
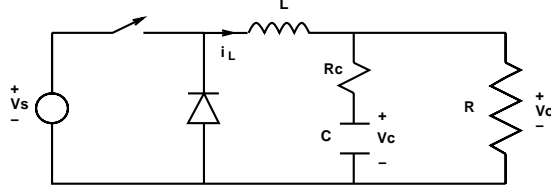
Figure 3: Buck converter with source voltage and resistive load

2.3 Boost Converter

The boost converter of interest in the paper is shown in Fig. 4. The matrices in Eq. (1) at each stage are

$$
\begin{aligned}
A_{\mathrm{ON}} &= A_{\mathrm{FF}} = \kappa \begin{bmatrix} 0 & 0 \\ 0 & -\omega_c \end{bmatrix}
& A_{\mathrm{OFF}} &= \kappa \begin{bmatrix} -\omega_l & -\omega_0 \\ \omega_0 & -\omega_c \end{bmatrix} \\
B_{\mathrm{ON}} &= B_{\mathrm{OFF}} = \begin{bmatrix} \frac{1}{\sqrt{L}} \\ 0 \end{bmatrix}
& B_{\mathrm{FF}} &= \begin{bmatrix} 0 \\ 0 \end{bmatrix} \\
E_{\mathrm{ON}} &= E_{\mathrm{FF}} = \kappa \begin{bmatrix} 0 & \frac{1}{\sqrt{C}} \end{bmatrix}
& E_{\mathrm{OFF}} &= \kappa \begin{bmatrix} \frac{R_c}{\sqrt{L}} & \frac{1}{\sqrt{C}} \end{bmatrix}
\end{aligned}
\tag{11}
$$
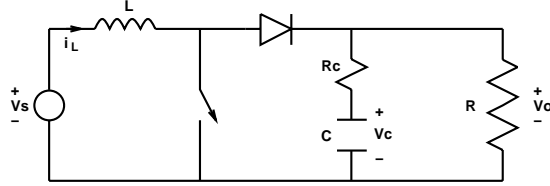
Figure 4: Boost converter with source voltage and resistive load

3 Sampled-Data Duty-Ratio-to-Output Transfer Functions for General PWM DC-DC Converters

In this section, the sampled-data duty-ratio-to-output transfer functions derived in [3] for *general* PWM DC-DC converters are recalled. For details, see [3].

Controlling the duty ratio is equivalent to controlling the switching instant within the cycle. In CCM, let the switching instant within the n-th cycle be $nT + d_n$. Let the seady-state value of d_n be d. Thus the steady-state duty ratio D_c is d/T in TEM, and $1 - d/T$ in LEM. Similarly in DCM,

there are two switching instants within the n-th cycle, let them be $nT + d_{1,n}$ and $nT + d_{2,n}$. The control signal in DCM is $d_{1,n}$, while $d_{2,n}$ is controlled internally by the inductor current. Let the seady-state values of $d_{1,n}$ and $d_{2,n}$ be d_1 and d_2, respectively.

The steady-state of $x(t)$ is generally a periodic solution (with a small ripple at high switching frequency), denoted as $x^0(t)$. Sampling $x^0(t)$ at $t = nT$ gives $x^0(0)$.

The steady-state values of $x^0(0)$, and d in CCM (or d_1, d_2 in DCM) can be obtained by solving a set of equations using the Newton's method. These values will be used in the derivation of poles and zeros.

Let the output of interest be the output voltage. This voltage is a time-varying signal. In the sampled-data model, it is sampled at each cycle. It has been shown in [3] that using the sampled output $v_o(nT + d_n)$ has better *phase* response than using the sampled output $v_o(nT)$. However, this makes the derivation of zeros more cumbersome. In the following, the sampled output $v_o(nT)$ is used.

The output voltage can be discontinuous. For example, this statement is true for the boost converter (Fig. 4) when $R_c \neq 0$ and therefore $E_{\text{ON}} \neq E_{\text{OFF}}$. In most applications, the output voltage of interest is the peak, minimum, or average voltage. In the following, E denotes E_1, E_2, or $(E_1 + E_2)/2$ in CCM; or E_1, E_3, $(E_1 + E_3)/2$ in DCM.

The dynamics for CCM and DCM differs. The duty-ratio-to-output transfer function for each mode is given next.

3.1 Continuous Conduction Mode (CCM)

The duty-ratio-to-output transfer function in CCM is

$$T_{oc}(z) = E(zI - \Phi_o)^{-1}\Gamma_d \cdot T \tag{12}$$

where

$$\Phi_o = \left.\frac{\partial f}{\partial x_n}\right|_\diamond = e^{A_2(T-d)}e^{A_1 d} \tag{13}$$

$$\Gamma_d = \left.\frac{\partial f}{\partial d_n}\right|_\diamond \quad = \quad e^{A_2(T-d)}((A_1 - A_2)x^0(d) + (B_1 - B_2)V_s)$$

$$= \quad e^{A_2(T-d)}(\dot{x}^0(d^-) - \dot{x}^0(d^+)) \tag{14}$$

Here $\dot{x}^0(d^-) = A_1 x^0(d) + B_1 V_s$ and $\dot{x}^0(d^+) = A_2 x^0(d) + B_2 V_s$ denote the time derivative of $x^0(t)$ at $t = d^-$ and d^+, respectively.

By omitting T in Eq. (12), it becomes the switching-instant-to-output transfer function, which has the same poles and zero as Eq. (12).

Given a transfer function in the z domain, say $T(z)$, its effective frequency response [14, p.93] is $T(e^{j\omega T})$, which is valid in the frequency range $|\omega| < \frac{\pi}{T}$. In the case when v_o is discontinuous due to $E_1 \neq E_2$, $T_{oc}(z)$ depends on which value of E is chosen.

In the two-dimensional cases (e.g., the buck converter in Fig. 3 and boost converter in Fig. 4), the transfer function (12) can be further simplified as (omitting T)

$$\frac{E(zI - \det[\Phi_o]\Phi_o^{-1})\Gamma_d}{\det[zI - \Phi_o]} = \frac{zE\Gamma_d - \det[\Phi_o]E\Phi_o^{-1}\Gamma_d}{\det[zI - \Phi_o]} \tag{15}$$

The poles are eigenvalues of Φ_o, denoted as $\sigma[\Phi_o]$. There always exists a zero (after substituting Φ_o and Γ_d from Eq. (13) and Eq. (14))

$$z_0 \quad = \quad \frac{\det[\Phi_o]E\Phi_o^{-1}\Gamma_d}{E\Gamma_d}$$

$$= \quad e^{\mathrm{tr}[A_2](T-d)+\mathrm{tr}[A_1]d}\frac{Ee^{-A_1 d}((A_1 - A_2)x^0(d) + (B_1 - B_2)V_s)}{Ee^{A_2(T-d)}((A_1 - A_2)x^0(d) + (B_1 - B_2)V_s)} \tag{16}$$

provided $Ee^{A_2(T-d)}((A_1 - A_2)x^0(d) + (B_1 - B_2)V_s) \neq 0$.

3.2 Discontinuous Conduction Mode (DCM)

The duty-ratio-to-output transfer function in DCM has the same form as in Eq. (12), but with

$$\Phi_o \quad = \quad e^{A_3(T-d_2)}(I - \frac{(\dot{x}^0(d_2^-) - \dot{x}^0(d_2^+))F}{F\dot{x}^0(d_2^-)})e^{A_2(d_2-d_1)}e^{A_1 d_1} \tag{17}$$

8

$$\Gamma_d = e^{A_3(T-d_2)}(I - \frac{(\dot{x}^0(d_2^-) - \dot{x}^0(d_2^+))F}{F\dot{x}^0(d_2^-)})e^{A_2(d_2-d_1)}(\dot{x}^0(d_1^-) - \dot{x}^0(d_1^+)) \tag{18}$$

where the matrix F is chosen such that $Fx = \sqrt{L}i_L$.

3.3 A Useful Fact

The following fact is useful for the derivation of poles and zeros. It can be verified using the Cayley-Hamilton theorem [15].

Fact 1 Let $A = \kappa \begin{bmatrix} -\omega_l & -\omega_0 \\ \omega_0 & -\omega_c \end{bmatrix}$ with $\omega_0 > \frac{|\omega_c - \omega_l|}{2}$, and let $\omega = \sqrt{\omega_0^2 - (\frac{\omega_c - \omega_l}{2})^2}$. Then

$$e^{At} = \frac{e^{\frac{-\kappa(\omega_c+\omega_l)t}{2}}}{\omega} \begin{bmatrix} (\frac{\omega_c-\omega_l}{2})\sin(\kappa\omega t) + \omega\cos(\kappa\omega t) & -\omega_0\sin(\kappa\omega t) \\ \omega_0\sin(\kappa\omega t) & (\frac{\omega_l-\omega_c}{2})\sin(\kappa\omega t) + \omega\cos(\kappa\omega t) \end{bmatrix} \tag{19}$$

4 Buck Converter in CCM

For the buck converter in CCM, the system matrices are given by

$$\begin{aligned} A_1 &= A_2 = A_{\text{ON}} \\ E &= E_{\text{ON}} \\ B_1 &= B_{\text{ON}}, \quad B_2 = 0_{2\times1} \quad \text{for trailing-edge modulation (TEM), while} \\ B_1 &= 0_{2\times1}, \quad B_2 = B_{\text{ON}} \quad \text{for leading-edge modulation (LEM)} \end{aligned} \tag{20}$$

4.1 Poles

The set of poles of the buck converter for either TEM or LEM is

$$\begin{aligned} \sigma[\Phi_o] &= \sigma[e^{A_{\text{ON}}T}] \qquad \text{(from Eqs. (13) and (20))} \\[2mm] &= e^{\kappa T(-\frac{\omega_c+\omega_l}{2}\pm j\omega)} \qquad \text{(from Eqs. (10) and (19))} \end{aligned} \tag{21}$$

4.2 Zero

The zero of the buck converter for either TEM or LEM is

$$z_0 = e^{-\kappa T(\omega_c+\omega_l)}\frac{Ee^{-A_{\text{ON}}d}B_{\text{ON}}V_s}{Ee^{A_{\text{ON}}(T-d)}B_{\text{ON}}V_s} \qquad \text{(from Eqs. (16) and Eq. (20))}$$

9

$$= e^{\frac{-\kappa T(\omega_c + \omega_l)}{2}} \frac{-\left(\frac{\omega_c - \omega_l}{2} + \omega_e\right)\sin(\kappa\omega d) + \omega\cos(\kappa\omega d)}{\left(\frac{\omega_c - \omega_l}{2} + \omega_e\right)\sin(\kappa\omega(T-d)) + \omega\cos(\kappa\omega(T-d))} \qquad \text{(from Eqs. (10) and (19))}$$

$$= e^{\frac{-\kappa T(\omega_c + \omega_l)}{2}} \frac{\sin(\kappa\omega d - \theta)}{\sin(\kappa\omega(d-T) - \theta)} \qquad (22)$$

where

$$\theta = \arctan\left(\frac{2\omega}{\omega_c - \omega_l + 2\omega_e}\right) \qquad (23)$$

Next, the zero is expressed in terms of the duty ratio. In TEM, $d = D_c T$, and Eq. (22) gives

$$z_0 = e^{\frac{-\kappa T(\omega_c + \omega_l)}{2}} \frac{\sin(\kappa\omega T D_c - \theta)}{\sin(\kappa\omega T(D_c - 1) - \theta)} \qquad (24)$$

In LEM, $d = (1 - D_c)T$, and Eq. (22) gives

$$z_0 = e^{\frac{-\kappa T(\omega_c + \omega_l)}{2}} \frac{\sin(\kappa\omega T(1 - D_c) - \theta)}{\sin(\kappa\omega T(-D_c) - \theta)} \qquad (25)$$

Therefore a buck converter with duty ratio D^* in TEM has the same zero as the same converter with duty ratio $(1 - D^*)$ in LEM. Due to this equivalence, only the TEM case is discussed in the following.

To show the effects of the duty ratio and the equivalent series resistance R_c on the location of the zero, the zero will be expressed as a function of D_c and R_c, viz. $z_0(D_c, R_c)$.

The following theorem applies to the function $z_0(D_c, R_c)$.

Theorem 1

(i) $z_0(D_c, 0) = e^{\frac{-T\omega_c}{2}} \frac{\sin(\omega T D_c)}{\sin(\omega T(D_c - 1))}$, *and therefore* $z_0(0, 0) = 0$

(ii) $z_0(0.5, 0) \in (-1, 0)$

(iii) If $\kappa\omega T \in (0, \pi)$, *then* $\frac{\partial}{\partial D_c} z_0(D_c, R_c) < 0$.

Thus the zero moves to the left in the complex plane as the duty ratio increases.

(iv) If $(\kappa\omega T + \theta) \in (0, \pi/2)$ *and* $(2\omega_e + \omega_c - \omega_l) > 0$, *then*

(iv.a) $z_0(0, R_c) \in [0, 1)$

(iv.b) $z_0(D_c, R_c) < 1$

(iv.c) $z_0(D_c, R_c) \geq z_0(D_c, 0)$

(iv.d) $z_0(D_c, R_c) \in (-1, 1)$ *for* $D_c < 0.5$.

From (iv.c), the ESR results in moving the zero to the right in the complex plane. From (iv.d), a sufficient condition for the zero to be stable is $D_c < 0.5$.

(v) If $\omega_s \gg \omega$ *and* $2\omega_e \gg (\omega_c - \omega_l)$, *then*

$$z_0(D_c, R_c) \approx \frac{\kappa T D_c - R_c C}{\kappa T(D_c - 1) - R_c C} \tag{26}$$

(The approximation becomes exact as ω_s *and* ω_e *grow without bound.) Thus a sufficient condition for the zero to be stable that holds for sufficiently large* ω_s *and* ω_e *is*

$$D_c < \frac{R_c C}{\kappa T} + \frac{1}{2} \tag{27}$$

If $R_c = 0$, *the zero is given by the approximate formula*

$$z_0(D_c, 0) \approx \frac{D_c}{D_c - 1} \tag{28}$$

Proof:

(i) For $R_c = 0$, $\omega_l = 0$, $\kappa = 1$, $\omega_e = \infty$ and $\theta = 0$ (from Eq. (23)). Then the statement follows from Eq. (24).

(ii) From *(i)*, $z_0(0.5, 0) = -e^{\frac{-\kappa T \omega_c}{2}} \in (-1, 0)$

(iii) Differentiating Eq. (24) with respect to D_c and using a trigonometric identity to simplify the result yields

$$\frac{\partial}{\partial D_c} z_0(D_c, R_c) = -e^{\frac{-\kappa T(\omega_c + \omega_l)}{2}} \frac{\kappa \omega T \sin(\kappa \omega T)}{\sin^2(\kappa \omega T(D_c - 1) - \theta)} < 0$$

(iv.a) From Eq. (23), if $(2\omega_e + \omega_c - \omega_l) > 0$, then $\theta \in [0, \pi/2)$. Now Eq. (24) gives

$$z_0(0, R_c) = e^{\frac{-\kappa T(\omega_c + \omega_l)}{2}} \frac{\sin(\theta)}{\sin(\kappa \omega T + \theta)} \in [0, 1)$$

11

$(iv.b)$ The conditions in (iv) imply that $\kappa \omega T \in (0, \pi)$, so the conclusion of (iii) applies. Thus,

$$z_0(D_c, R_c) \quad < \quad z_0(0, R_c) \quad \text{(from } (iii))$$

$$< \quad 1 \quad \text{(from } (iv.a))$$

$(iv.c)$ From Eq. (24),

$$z_0(D_c, R_c) - z_0(D_c, 0)$$

$$= \quad e^{\frac{-\kappa T(\omega_c + \omega_l)}{2}} \left(\frac{\sin(\kappa \omega T D_c - \theta)}{\sin(\kappa \omega T (D_c - 1) - \theta)} - \frac{\sin(\kappa \omega T D_c)}{\sin(\kappa \omega T (D_c - 1))} \right)$$

$$= \quad e^{\frac{-\kappa T(\omega_c + \omega_l)}{2}} \frac{\cos(\kappa \omega T - \theta) - \cos(\kappa \omega T + \theta)}{2 \sin(\kappa \omega T (D_c - 1) - \theta) \sin(\kappa \omega T (D_c - 1))}$$

$$= \quad e^{\frac{-\kappa T(\omega_c + \omega_l)}{2}} \frac{\sin(\kappa \omega T) \sin(\theta)}{\sin(\kappa \omega T (1 - D_c) + \theta) \sin(\kappa \omega T (1 - D_c))}$$

$$\geq \quad 0$$

$(iv.d)$ For $D_c < 0.5$,

$$z_0(D_c, R_c) \quad > \quad z_0(0.5, R_c) \quad \text{(from } (iii))$$

$$\geq \quad z_0(0.5, 0) \quad \text{(from } (iv.c))$$

$$> \quad -1 \quad \text{(from } (ii))$$

(v) If $2\omega_e \gg (\omega_c - \omega_l)$, Eq. (23) gives $\theta \approx \arctan(\frac{\omega}{\omega_e}) \approx \frac{\omega}{\omega_e}$. If $\omega_s \gg \omega$, then ωT is small. Thus Eq. (24) gives

$$z_0(D_c, R_c) \quad \approx \quad \frac{\kappa \omega T D_c - \theta}{\kappa \omega T (D_c - 1) - \theta}$$

$$\approx \quad \frac{\kappa \omega T D_c - \frac{\omega}{\omega_e}}{\kappa \omega T (D_c - 1) - \frac{\omega}{\omega_e}}$$

$$= \quad \frac{\kappa T D_c - R_c C}{\kappa T (D_c - 1) - R_c C}$$

$\square$

In summary, the zero of the buck converter is a real number that depends on the switching frequency and the duty ratio, as well as on the modulation scheme (viz., TEM or LEM). The quantity is always less than 1, but the zero can be unstable (if it is less than -1). The effect of the ESR is to move the zero to the right in the complex plane.

In TEM, the zero moves to the left in the complex plane as the duty ratio increases. It lies within the unit circle if the duty ratio is less than 0.5. In LEM, the zero moves to the right in the complex plane as the duty ratio increases. The zero lies within the unit circle if the duty ratio is greater than 0.5.

Although it has been shown above that the buck converter sampled-data model can have an unstable zero, no experimental observation of undershoot (a common phenomenon for system with unstable zero) has, to the author's knowledge, been reported for a buck converter. This can be explained as follows. In a linear discrete-time system, an initial undershoot will occur if and only if the system has an odd number of real *positive* unstable zeros [16, 17]. Since any unstable zero of the buck converter sampled-data model will be real and *negative*, this explains why undershoot has never been observed in the buck converter.

5 Boost Converter in CCM

Derivation of poles or the zero of a boost converter is more complicated than that for a buck converter because $A_{\mathrm{ON}} \neq A_{\mathrm{OFF}}$ for a boost converter.

5.1 Poles

From Eq. (13), the set of poles of the boost converter for either TEM or LEM is

$$
\begin{aligned}
\sigma[\Phi_o] &= \sigma[e^{A_{\mathrm{OFF}}T(1-D_c)}e^{A_{\mathrm{ON}}TD_c}] \\
&:= p_0,\ p_0^*
\end{aligned}
\tag{29}
$$

where the notation p_0 and p_0^* is used, since the system is 2-dimensional and usually the eigenvalues occur in a complex conjugate pair. The poles can be calculated numerically from this equation. In

13

the following, the poles will be estimated in compact form.

For $\omega_s \gg \omega_0$, then $e^{A_{\mathrm{ON}}TD_c} \approx I$. From Eqs. (29), (19) and (11), one has

$$
\begin{aligned}
p_0, \ p_0^* \quad &\approx \quad \sigma[e^{A_{\mathrm{OFF}}T(1-D_c)}] \\[2mm]
&= \quad e^{\kappa T(1-D_c)(-\frac{\omega_c+\omega_l}{2}\pm j\omega)} \qquad \text{(from Eqs. (10) and (19))} \\[2mm]
&:= \quad p_{e1}, \ p_{e1}^* \hspace{5cm} (30)
\end{aligned}
$$

From Eqs. (29) and (30), the estimated pole p_{e1} and the true pole p_0 are related by

$$
\begin{aligned}
\frac{|p_0|}{|p_{e1}|} \quad &= \quad \frac{\sqrt{\det[e^{A_{\mathrm{ON}}TD_c}e^{A_{\mathrm{OFF}}T(1-D_c)}]}}{\sqrt{\det[e^{A_{\mathrm{OFF}}T(1-D_c)}]}} \\[3mm]
&= \quad \sqrt{\det[e^{A_{\mathrm{ON}}TD_c}]} \\[3mm]
&= \quad e^{\frac{-\kappa\omega_c TD_c}{2}} \qquad \text{(from Eq. (11))} \\[3mm]
&< \quad 1
\end{aligned}
$$

From Fig. 5, it can be proved that $|p_{e2} - p_0| < |p_{e1} - p_0|$ by geometric arguments. Therefore a better estimate of the pole is

$$
\begin{aligned}
p_{e2} \quad &= \quad \frac{|p_0|}{|p_{e1}|}p_{e1} \\[3mm]
&= \quad e^{\frac{-\kappa\omega_c TD_c}{2}}p_{e1} \\[3mm]
&= \quad e^{\frac{-\kappa\omega_c TD_c}{2}+\kappa T(1-D_c)(-\frac{\omega_c+\omega_l}{2}\pm j\omega)} \\[3mm]
&= \quad e^{\frac{-\kappa T\omega_c}{2}+\kappa T(1-D_c)(-\frac{\omega_l}{2}\pm j\omega)} \hspace{3cm} (31)
\end{aligned}
$$

which has the same magnitude as the true pole p_0.

In the following, the pole p_{e2} is transformed to the continuous-time domain and is compared with the pole from the averaging method. For simplicity, only the case $R_c = 0$ is shown. In this case, the poles in the continuous-time domain are

$$
p_{e2}^c \quad := \quad \frac{1}{T}\ln[p_{e2}]
$$
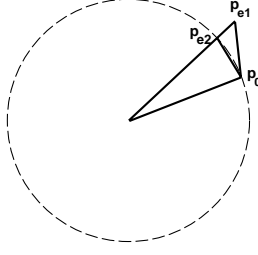
Figure 5: The estimated pole p_{e2} gives a better estimate of the true pole p_0 than p_{e1}

$$= -\frac{\omega_c}{2} \pm j(1 - D_c)\omega$$

$$= -\frac{\omega_c}{2} \pm j\sqrt{(1 - D_c)^2\omega_0^2 - (1 - D_c)^2\frac{\omega_c^2}{4}} \tag{32}$$

From [9, p.293], the continuous-time poles calculated from averaging method are

$$-\frac{1}{2RC} \pm j\sqrt{\frac{(1 - D_c)^2}{LC} - \frac{1}{4R^2C^2}} = -\frac{\omega_c}{2} \pm j\sqrt{(1 - D_c)^2\omega_0^2 - \frac{\omega_c^2}{4}} \tag{33}$$

The poles calculated from the sampled-data method and averaging method, Eqs. (32) and (33), are very close. Experimental work is needed to verify which one is more accurate.

5.2   Zero

The zero is derived exactly for the case $R_c = 0$, and approximatedly for the case $R_c \neq 0$.

For the case $R_c = 0$, $\omega_l = 0$ and $\kappa = 1$. The system matrices in Eq. (11) at ON and OFF stages becomes

$$
\begin{aligned}
A_{\mathrm{ON}} &= \begin{bmatrix} 0 & 0 \\ 0 & -\omega_c \end{bmatrix} & A_{\mathrm{OFF}} &= \begin{bmatrix} 0 & -\omega_0 \\ \omega_0 & -\omega_c \end{bmatrix} \\
B_{\mathrm{ON}} &= B_{\mathrm{OFF}} = \begin{bmatrix} \frac{1}{\sqrt{L}} \\ 0 \end{bmatrix} \\
E_{\mathrm{ON}} &= E_{\mathrm{OFF}} = \begin{bmatrix} 0 & \frac{1}{\sqrt{C}} \end{bmatrix}
\end{aligned}
\tag{34}
$$

Since $E_{\mathrm{ON}} = E_{\mathrm{OFF}}$, the output voltage is continuous.

The zero of the boost converter model in TEM is

$$z_0 = e^{\text{tr}[A_{\text{OFF}}](T-d)+\text{tr}[A_{\text{ON}}]d} \frac{E_{\text{ON}}e^{-A_{\text{ON}}d}(A_{\text{ON}}-A_{\text{OFF}})x^0(d)}{E_{\text{ON}}e^{A_{\text{OFF}}(T-d)}(A_{\text{ON}}-A_{\text{OFF}})x^0(d)} \qquad \text{(from Eq. (16))}$$

$$= \frac{e^{\frac{-\omega_c T(1-D_c)}{2}}}{\cos(\omega T(1-D_c)) - \frac{\sin(\omega T(1-D_c))}{\omega}(\frac{\omega_c}{2} + \frac{v_c(TD_c)}{Li_L(TD_c)})} \qquad \text{(from Eqs. (34) and (19))}$$

The value of $\frac{v_c(TD_c)}{i_L(TD_c)}$ can be approximated by $(1-D_c)R$ [9]. Then for $\omega_s \gg \omega$ and $R \gg \sqrt{L/C}$,

$$z_0 \approx \frac{1}{1 - \frac{T(1-D_c)^2 R}{L}} \tag{35}$$

Based on this approximation, the zero is stable if $D_c < 1 - \sqrt{\frac{2L}{TR}}$ and is positive if $D_c > 1 - \sqrt{\frac{L}{TR}}$.

Similarly, the zero of the boost converter with $R_c = 0$ in LEM is

$$e^{\frac{-\omega_c T(1-D_c)}{2}}(\cos(\omega T(1-D_c)) + \frac{\sin(\omega T(1-D_c))}{\omega}(\frac{\omega_c}{2} + \frac{v_c(T(1-D_c))}{Li_L(T(1-D_c))}))$$

$$\approx 1 + \frac{T(1-D_c)^2 R}{L} \quad \text{for } \omega_s \gg \omega_0 \text{ and } R \gg \sqrt{\frac{L}{C}} \tag{36}$$

which is positive and unstable.

In the case $R_c \neq 0$, the output voltage is discontinuous. Use $Ex = \frac{1}{2}(E_{\text{ON}} + E_{\text{OFF}})x$ to approximate the average output voltage. Similar to previous analysis, the zero of the boost converter with $R_c \neq 0$ in TEM is approximately

$$\frac{\frac{R_c}{2}\sqrt{\frac{C}{L}}\frac{R(1-D_c)}{L} - \omega_0}{\frac{R_c}{2}\sqrt{\frac{C}{L}}(\frac{R(1-D_c)}{L} + \omega_0^2 T(1-D_c)) + \frac{\omega_0 TR(1-D_c)^2}{L} - \omega_0} \tag{37}$$

and the zero of the boost converter with $R_c \neq 0$ in LEM is approximately

$$\frac{\frac{R_c}{2}\sqrt{\frac{C}{L}}\frac{R(1-D_c)}{L} - \frac{\omega_0 TR(1-D_c)^2}{L} - \omega_0}{\frac{R_c}{2}\sqrt{\frac{C}{L}}\frac{R(1-D_c)}{L} - \omega_0} \tag{38}$$

6 Buck and Boost Converters in DCM

It has been shown in [3] that the dynamics of the buck or boost converter in DCM is 1-dimensional. Although the state is expressed as $x_n=(\sqrt{L}i_{L,n}, \sqrt{C}v_{C,n})$, the state $\sqrt{L}i_{L,n}$ is always 0, which makes one pole to be 0 and therefore $\det[\Phi_o] = 0$. From Eq. (15), the zero is at 0, and it is canceled by the pole at 0. Thus there is only one pole but no more zero. This pole corresponds to the state $\sqrt{C}v_{C,n}$, and it is $\Phi_o(2,2)$ (i.e. the component in the second column and second row of Φ_o).

As shown in Eq. (17), the matrix Φ_o consists of 4 parts multiplied together. The first 2 parts are the same for the buck and boost converter. They are

$$e^{A_3(T-d_2)} = \begin{bmatrix} 1 & 0 \\ 0 & e^{-\kappa\omega_c(T-d_2)} \end{bmatrix} \tag{39}$$

$$I - \frac{(\dot{x}^0(d_2^-) - \dot{x}^0(d_2^+))F}{F\dot{x}^0(d_2^-)} = I + \begin{bmatrix} -1 & 0 \\ \frac{\sqrt{C}(\dot{v}_C(d_2^+)-\dot{v}_C(d_2^-))}{\sqrt{L}i_L(d_2^-)} & 0 \end{bmatrix}$$

$$= \begin{bmatrix} 0 & 0 \\ 0 & 1 \end{bmatrix} \tag{40}$$

The last equation follows from $\dot{v}_C(d_2^+) - \dot{v}_C(d_2^-) = -\kappa\omega_c(v_C(d_2) - v_C(d_2)) = 0$.

From Eqs. (17), (39) and (40), one has

$$\Phi_o(2,2) = e^{-\kappa\omega_c(T-d_2)} \cdot (\text{the (2,2) component of } e^{A_2(d_2-d_1)}e^{A_1d_1}) \tag{41}$$

The pole, $\Phi_o(2,2)$, of the buck and boost converters will be further derived in the following two subsections.

In a continuous-time system (for example, the averaged model), a transfer function with one pole can not have phase response beyond -90 degrees. However, in a discrete-time system, a transfer function with one pole can have phase response beyond -90 degrees.

6.1 Pole of Buck Converter

From Eqs. (41), (10) and (19), the pole of the buck converter is

$$e^{-\kappa\omega_c(T-\frac{d_2}{2})}e^{-\kappa\omega_l(\frac{d_2}{2})}((\frac{\omega_l-\omega_c}{2\omega})\sin(\kappa\omega d_2)+\cos(\kappa\omega d_2)) \tag{42}$$

Using the function $\frac{1}{T}\ln[\cdot]$ to transform this pole for the discrete-time to the continuous-time domain, the pole becomes

$$-\kappa\omega_c(1-\frac{d_2}{2T})-\kappa\omega_l(\frac{d_2}{2T})+\frac{1}{T}\ln[(\frac{\omega_l-\omega_c}{2\omega})\sin(\kappa\omega d_2)+\cos(\kappa\omega d_2)] \tag{43}$$

6.2 Pole of Boost Converter

From Eqs. (41), (11) and (19), the pole of the boost converter is

$$e^{-\kappa\omega_c(T-\frac{d_2-d_1}{2})}e^{-\kappa\omega_l(\frac{d_2-d_1}{2})}((\frac{\omega_l-\omega_c}{2\omega})\sin(\kappa\omega(d_2-d_1))+\cos(\kappa\omega(d_2-d_1))) \tag{44}$$

Using the function $\frac{1}{T}\ln[\cdot]$ to transform this pole for the discrete-time to the continuous-time domain, the pole becomes

$$-\kappa\omega_c(1-\frac{d_2-d_1}{2T})-\kappa\omega_l(\frac{d_2-d_1}{2T})+\frac{1}{T}\ln[(\frac{\omega_l-\omega_c}{2\omega})\sin(\kappa\omega(d_2-d_1))+\cos(\kappa\omega(d_2-d_1))] \tag{45}$$

7 Illustrative Examples

Example 1 (*Zero of the buck converter in CCM*, [11, p.326]) The system parameters are $f_s = 200kHz$, $V_s = 8V$, $R = 0.2\Omega$, $L = 5\mu H$, $C = 2mF$, and $R_c = 0.01\Omega$. Eqs. (24) and (25) are used to plot the location of the zero for TEM and LEM respectively as the duty ratio varies. The plot is shown in Fig. 6. If the ESR is not included in the model (i.e.,$R_c = 0$), the location of the zero is as shown in Fig. 7. The effect of ESR can be seen: for the same duty ratio, the zero in case $R_c \neq 0$ lies to the right in the complex plane of the zero in case $R_c = 0$.

Example 2 (*Zero of the boost converter in CCM*, [18]) The system parameters are $f_s = 25kHz$, $V_s = 20V$, $R = 17\Omega$, $L = 350\mu H$, $C = 660\mu F$, and $R_c = 0.075\Omega$. It is claimed in [18] that if,
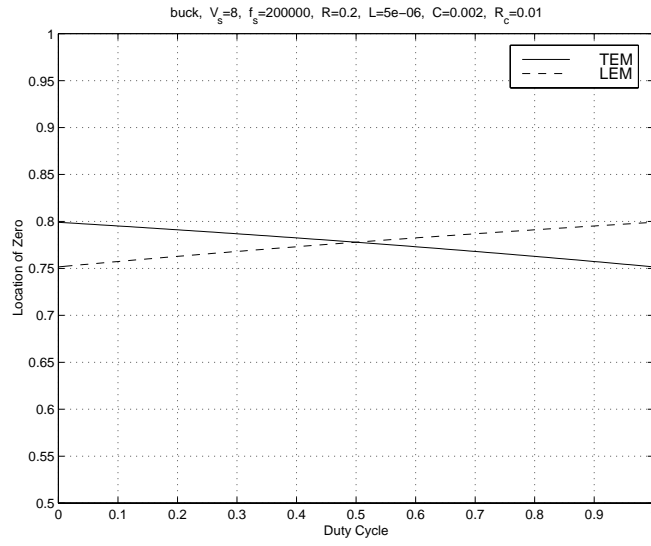
Figure 6: Zero of the buck converter in TEM and LEM as the duty ratio varies when $R_c = 0.01\Omega$
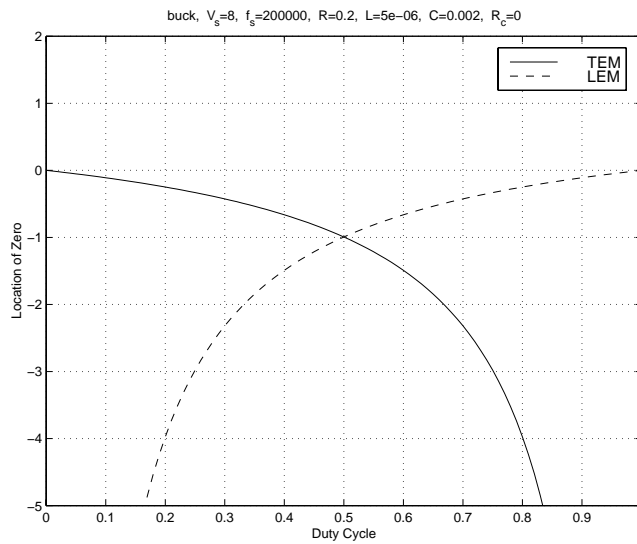
Figure 7: Zero of the buck converter in TEM and LEM as the duty ratio varies when $R_c = 0$

19

instead of TEM, LEM is used and if the condition

$$D_c < 1 - \frac{L}{RR_cC} \tag{46}$$

is satisfied, then the unstable zero of the boost converter in TEM is removed.

Let $D_c = 0.3$, which satisfies this condition. Since the output voltage is discontinuous, $Ex = \frac{1}{2}(E_{\text{ON}} + E_{\text{OFF}})x$ is used to approximate the average output voltage. From Eq. (16), the zero in TEM and LEM, respectively, is calculated as -0.4495 and 99.4607 respectively. Therefore it is expected that if there is a step increase in the duty ratio, the time response of average output voltage will not undergo undershoot in TEM, while it will in LEM. This result is the exact opposite of that in [18]. Not only can LEM not remove the unstable zero, but it also does not result in a better performance than TEM. Fig. 8 and Fig. 9 show the output voltage in TEM and LEM respectively when the duty ratio is changed from 0.3 to 0.45. In these figures, undershoot arises both in TEM and LEM. If the sampled mid-value output voltage $Ex(nT)$, deonted by the symbol ○ in the figures, is concentrated, then it exhibits a small undershoot in LEM while it exhibits no undershoot in TEM. The undershoot of average output voltage in LEM is very small because the unstable positive zero (99.4607) is far from 1.

Example 3 (*Boost converter in DCM*, [19]) The system parameters are $f_s = 100kHz$, (thus $T = 10\mu$ seconds), $V_s = 5V$, $R = 20\Omega$, $L = 5\mu H$, $C = 40\mu F$, $R_c = 0$ and $d_1 = 0.7T$.

Through the steady-state analysis stated in [3], the following steady-state values are obtained: $d_2 = 0.9616T$, $x^0(0) = (0, 0.1165)$, $x^0(d_1) = (0.0157, 0.1155)$ and $x^0(d_2) = (0, 0.1165)$.

From Eq. (44), the pole in the sampled-data domain is 0.9707. From Eq. (45), the pole in the continuous-time domain is -2972.6.

Using Eqs. (12), (17) and (18), the frequency response is shown as a solid line in Fig. 11. In [19], a 2-dimensional model for DCM is proposed. For comparison, the frequency responses of this model is shown as a dashed line in Fig. 11. The sampled-data model agrees very well with the proposed model in [19], where the latter has been shown to agree with the results by SABER simulations [19].
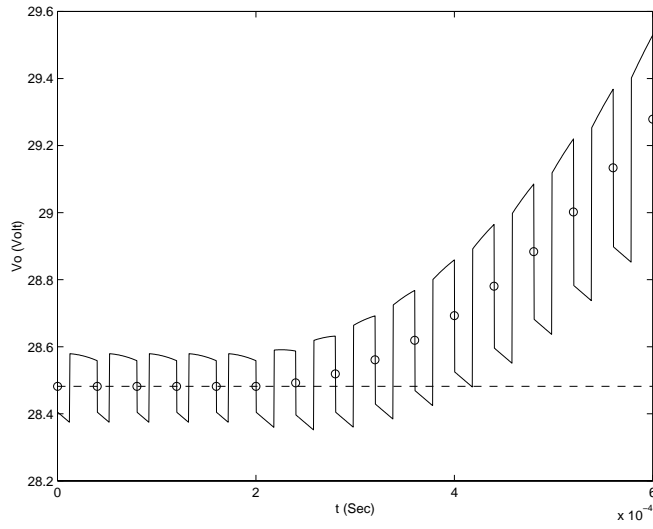
Figure 8: Transient output voltage response in TEM when the duty ratio is changed from 0.3 to 0.45 at $t = 2 \times 10^{-4}$; the symbol $\circ$ denotes $\frac{1}{2}(E_{\mathrm{ON}} + E_{\mathrm{OFF}})x(nT)$
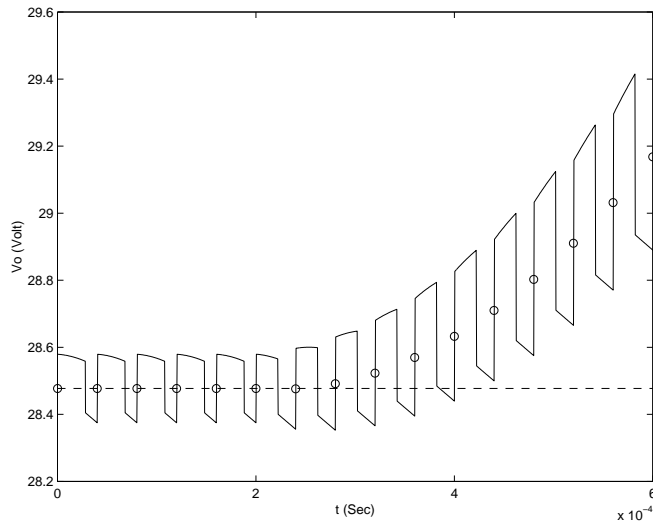
Figure 9: Transient output voltage response in LEM when the duty ratio is changed from 0.3 to 0.45 at $t = 2 \times 10^{-4}$; the symbol $\circ$ denotes $\frac{1}{2}(E_{\mathrm{ON}} + E_{\mathrm{OFF}})x(nT)$
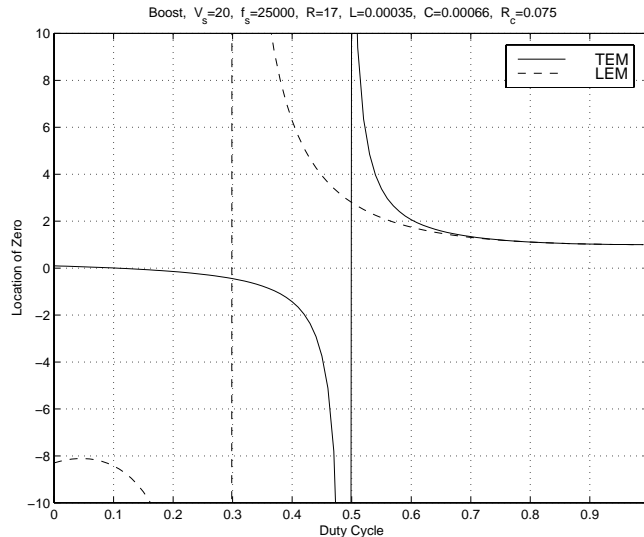
Figure 10: Zero location in TEM and LEM as the duty ratio varies

The following remarks resolves the issue on how many poles in a converter operating in DCM. There is only one pole and no zero in the *sampled-data* dynamics of the boost converter in DCM. The phase of the duty-ratio-to-output transfer function of the sampled-data model can go beyond -90 degrees, although there is only one pole. This agrees with the experimental observation in [20].

8   Concluding Remarks

Poles and zeros for sampled-data models of buck and boost converters are derived analytically for the first time (to the author's knowledge). This work employs recent work of the author on sampled-data modeling and analysis of PWM DC-DC converters [1, 2, 3].

Comparisons are made between the sampled-data and the averaged models. For poles, the two models give similar results except in the DCM operation. For zeros, however, the two models give quite different results.

In the sampled-data model of the PWM converter, the open-loop zero differs from that obtained for the averaged model. The zero derived from the sampled-data model depends on the switching frequency and duty ratio, as well as on the modulation scheme (viz., TEM or LEM).

For the buck converter in CCM, a zero exists even if the ESR is not modeled. Inclusion of the
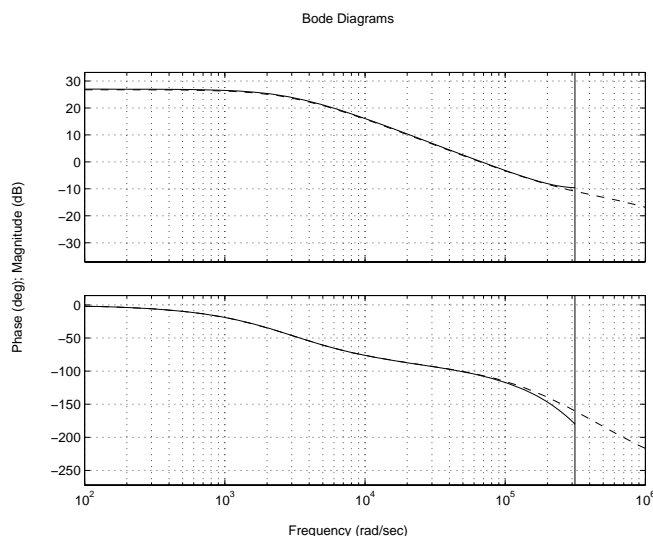
Figure 11: Frequency responses for the sampled-data model (solid line) and the model proposed in [18] (dashed line)

ESR in the model results in shifting the zero to the right in the complex plane. The zero can be unstable with or without the ESR being modeled. Undershoot is not observed because the zero is less than 1.

For the boost converter in CCM, only one zero exists and this zero can be stable when the duty ratio is small. LEM does not necessarily result in better performance than TEM even if the condition (46) guaranteeing a stable zero is satisfied.

For the buck or boost converter in DCM, only one pole exists and there is no zero. The phase frequency response can go beyond -90 degrees. This differs from the single-pole continuous-time system (e.g., averaged model), whose phase frequency response can not go beyond -90 degrees.

Acknowledgments

References

[1] C.-C. Fang and E.H. Abed, "Sampled-data modeling and analysis of closed-loop PWM DC-DC

converters," to appear at *IEEE International Symposium on Circuits and System*, May 1999.

[2] C.-C. Fang and E.H. Abed, "Sampled-data modeling and analysis of PWM DC-DC converters I. Closed-loop circuits," Tech. Rep. 98-54, Institute for Systems Research, University of Maryland, College Park, 1998, available at http://www.isr.umd.edu/TechReports/ISR/1998/.

[3] C.-C. Fang and E.H. Abed, "Sampled-data modeling and analysis of PWM DC-DC converters II. The power stage," Tech. Rep. 98-55, Institute for Systems Research, University of Maryland, College Park, 1998, available at http://www.isr.umd.edu/TechReports/ISR/1998/.

[4] F. Garofalo, P. Marino, S. Scala, and F. Vasca, "Control of DC-DC converters with linear optimal feedback and nonlinear feedforward," *IEEE Transactions on Power Electronics*, vol. 9, no. 6, pp. 607–615, 1994.

[5] C.-C. Fang and E.H. Abed, "Output regulation of DC-DC switching converters using discrete-time integral control," to appear at *American Control Conference*, June 1999.

[6] C.-C. Fang and E.H. Abed, "Discrete-time integral control of PWM DC-DC converters," Tech. Rep. 98-52, Institute for Systems Research, University of Maryland, College Park, 1998, available at http://www.isr.umd.edu/TechReports/ISR/1998/.

[7] R.D. Middlebrook and S. Ćuk, "A general unified approach to modelling switching-converter power stages," in *IEEE Power Electronics Specialists Conference Record*, 1976, pp. 18–34.

[8] S. Ćuk and R.D. Middlebrook, "A general unified approach to modelling switching DC-to-DC converters in discontinuous conduction mode," in *IEEE Power Electronics Specialists Conference Record*, 1977, pp. 36–57.

[9] R.W. Erickson, *Fundamentals of Power Electronics*, Chapman and Hall, New York, 1997.

[10] D.J. Shortt and F.C. Lee, "Extensions of the discrete average models for converter power stages," *IEEE Transactions on Aerospace and Electronic Systems*, vol. 20, no. 3, pp. 279–289, 1984.

[11] N. Mohan, T.M. Undeland, and W.P. Robbins, *Power Electronics: Converters, Applications, and Design*, Wiley, New York, 1995.

[12] K.H. Billings, *Switchmode Power Supply Handbook*, McGraw-Hill, New York, 1989.

[13] D.M. Mitchell, *DC-DC Switching Regulator Analysis*, McGraw-Hill, New York, 1988.

[14] A.V. Oppenheim and R.W. Schafer, *Discrete-Time Signal Processing*, Prentice-Hall, Englewood Cliffs, NJ, 1989.

[15] Stephen H. Friedberg, Arnold J. Insel, and Lawrence E. Spence, *Linear algebra*, Prentice-Hall, Upper Saddle River, NJ, Third edition, 1997.

[16] G. Deodhare and M. Vidyasagar, "Control system design via infinite linear programming," *International Journal of Control*, vol. 55, no. 6, pp. 1351–1380, 1992.

[17] B.L. de La Barra, M. El-Khoury, and M. Fernandez, "On undershoot in scalar discrete-time systems," *Automatica*, vol. 32, no. 2, pp. 255–259, 1996.

[18] D.M. Sable, B.H. Cho, and R.B. Ridley, "Elimination of the positive zero in fixed frequency boost and flyback converters," in *Fifth Annual Applied Power Electronics Conference and Exposition*, 1990, pp. 205–211.

[19] J. Sun, D.M. Mitchell, M. Greuel, P.T. Krein, and R.M. Bass, "Modeling of PWM converters in discontinuous conduction mode - A reexamination," in *IEEE Power Electronics Specialists Conference Record*, 1998.

[20] V. Vorperian, "Simplified analysis of PWM converters using model of PWM switch. II. Discontinuous conduction mode," *IEEE Transactions on Aerospace and Electronic Systems*, vol. 26, no. 3, pp. 497–505, 1990.